JCTC Journal of Chemical Theory and Computation

Article

pubs.acs.org/JCTC

Configurational Behavior and Conductance of Alkanedithiol Molecular Wires from Accelerated Dynamics Simulations

S. Alexis Paz, Martin E. Zoloff Michoff, Christian F. A. Negre, Jimena A. Olmos-Asar, Marcelo M. Mariscal, Cristián G. Sánchez, and Ezequiel P. M. Leiva*

Departamento de Matemática y Física, Facultad de Ciencias Químicas, Universidad Nacional de Córdoba, Córdoba

Supporting Information

ABSTRACT: An accelerated dynamics scheme is employed to sample the configurational space of a system consisting of an alkanedithiol molecule confined to the gap between a metal tip and a perfect metal surface. With this information and by means of nonequilibrium green functions techniques (NEGF), conductance calculations are performed. The present results show that even for this system, which is one of the most simple conceivable because of the perfectness of the surface, a complex behavior appears due to the occurrence of an unexpected tip-molecule-surface arrangement, where the insertion of one of the molecular ends into the tip−surface gap generates configurations with strongly enhanced conductance. Estimates are also made for the time required to generate the molecular junction, indicating that it should depend on the tip−surface distance, thus opening the way to new experiments in this direction.

1. INTRODUCTION

The miniaturization of electronic components has no choice but to reach molecular levels; thus, employing single molecules as new electronic components should become crucial in the near future. These nanometric systems exhibit different $I-V$ characteristics, providing a great potential versatility for the design of electronic devices.[1−4] However, for this to be experimentally accessible, it is mandatory to solve several problems such as controlling the coupling to contacts,[5,6] reducing eletron-phonon interactions,[7] and finding a gating mechanism to control current flow,[8] just to mention a few.

In an effort to understand the transport properties of single molecules, several studies describing molecules trapped in between two metal nanocontacts have been carried out.[7,9−17] In most cases, transport properties have been the analyzed feature, although some progress has been made regarding single molecule mechanical properties.[18−21] The most simple and challenging system appears to be the one formed by an alkanedithiol molecule trapped between two Au nanotips. The electromechanical behavior of this system has shown to be difficult to understand, and the wide range of disparate results reported in the literature makes this understanding even harder.[22] Depending on the experimental method employed, repeated conductance measurements show histograms with more than one peak. This is the case of the measurements performed in refs 9, 12, and 23, where three fundamental conductance peaks were found. Haiss et al.[23] have attributed the three fundamental conductance contributions to different types of contacts of the molecule with the metal surfaces, namely a loose contact with the tip and the surface, thiol adsorption at step edges, and attachment of both sulfur headgroups to step edges. While the first type of contacts should be favored in the case of the so-called $I(t)$ type of experiments,[14] where one of the ends of the molecule is picked by a STM tip held at a constant distance from the surface, the other two would arise when a close interaction of the tip with the surface is allowed or when the surface shows a preexistent important number of defects. Thus, it would appear that the most simple system is provided by the $I(t)$ experiments, involving a single molecule confined between a metal tip and a (more or less) perfect surface.

Different theoretical approaches have been undertaken to understand the behavior of Au−dithiol−Au junctions. To explain the temperature dependence of conductance, tunneling models have been proposed that consider configurations where the maximum of conductance does not correspond to the minimum energy molecular configuration.[4,24,25] Thus, extensive configuration sampling of the junction is needed to find those structures that could strongly contribute to the conductance but may not be thermodynamically favored. In this respect, efforts have been made to perform these averages through molecular dynamics (MD) and conformational searches.[26,27] On the basis of these pioneering articles, the obvious choice appears to be the use of computer simulations to get molecular configurations that can be used to calculate electronic transport properties of the system. For this approach to be valid, an extensive sampling of the molecular configurations at the tip−surface gap is required. Such an approach has been already taken elsewhere for a relatively simple molecular system (p-benzene dithiol) with promising results.[28] However, one of the factors precluding the straightforward comparison of results stemming from molecular dynamics with experiments in the case of alkanedithiols are the time scales where both approaches are developed.

While conductance measurements are usually in the time scale of the millisecond, where the molecules may access a manyfold of conformers, computer simulations usually reach time scales several order of magnitude smaller. In this respect, the application of simulation schemes that allow to study

Received: August 23, 2012
Published: October 8, 2012

   dx.doi.org/10.1021/ct3007327 | J. Chem. Theory Comput. 2012, 8, 4539−4545

phenomena well beyond the nanosecond range are mandatory. Motivated by this challenge, in this work, we apply accelerated molecular dynamics (AMD) combined with electronic transport simulations based on nonequilibrium Green functions techniques (NEGF) with which we are able to reproduce the main experimental features of a conductance histogram for a octanodithiol molecule trapped in between Au clusters simulating a STM tip and a Au(111) surface. Besides these calculations, we also use some resources from accelerated dynamics such as the nudged elastic band (NEB), in order to raise some questions that will open new directions for research on this interesting and still not completely understood phenomenon.

2. METHODOLOGY

2.1. Semiemprical Description. To formulate a representative model of the molecule trapped in the tip−surface junction, we employ an atomistic description of the system amounting a total of 873 atoms, 26 of which correspond to the octanedithiol molecule and the rest to gold atoms. From the latter, 672 belong to the surface, which is assumed to be infinite through peridic boundary conditions in the $x-y$ direction. A scheme of the geometric arrangement of the system is given in Figure 1. Accordingly, a suitable semiempirical description must

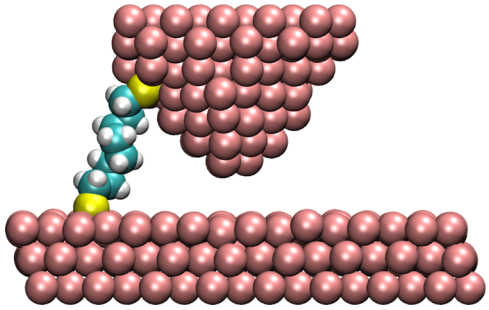

Figure 1. Scheme of the atomistic model employed in the present simulations. Au atoms are shown in pink, S in yellow, C in blue, and H in white. The upper and bottom layer of Au atoms were kept fixed during the atom dynamics simulations. All atoms were included in the calculation of the conductance of the system.

be chosen to make the computations feasible in a reasonable amount of computer time. With this purpose, for the molecule-metal interaction we use a recently proposed semiempirical potential,[29] based on density functional calculations and a bond-order Morse-like potential. This potential was developed to simulate the adsorption behavior of thiolate molecules on nonplanar gold surfaces, including relaxing effects. Its functional form includes as variables the metal-molecule separation, vibrational motions, bending and torsion angles between several pairs of atom types, and the coordination number of both the metal (Au) and thiolate groups. This potential was parametrized based on a set of density functional calculations of molecular adsorption on several surface sites (i.e., hollow, bridge, top, on-top Au adatom, and the novel staple motif) for different Au(111) and (100) crystalline faces and delivers results in very good agreement with experimental results. The intramolecular interactions of the octanedithiol molecule were represented using the all-atom optimized potentials for liquid simulations (OPLS-AA) force field. The parameters used for the simulations were extracted from ref 30. In the case of the metal−metal interaction, the present choice is the potential due to the second-moment approximation of tight binding (SMTB), which takes into account the many-body character of the metallic bond and has been found to reproduce most of the characteristic properties of gold. The parameters of this potential where taken from ref 31.

The substrate surface was represented using a perfect Au (111) surface containing three atomic layers. On the other hand, the tip was made by stretching a 400 atoms gold cube with fcc structure from two of its opposite faces until rupture at a rate of 2 Å/ps. For all the simulation methods, the top and bottom gold layers were fixed at their bulk lattice positions. The tip, the molecule, and the surface were assembled together, and then an up−down tip motion cycle was performed with a rate of 2 Å/ps at constant temperature (300 K) using the Ermak thermostat. This was the default temperature control adopted in all the simulations of the present work. The cycle ended at the tip−surface distance at which the configuration sampling was performed, and before each sampling the system was thermalized at 300 K for 1.5 ns.

2.2. NEB Calculations. Activation energies and minimum energy paths were obtained from nudged elastic band (NEB) calculations.[32] The NEB method was applied considering different numbers of images (50, 100, 200, 500, and 1000) and spring constant values (5, 50, and 100 eV Å^{-2}). Different combinations of these parameters yielded essentially the same results. We report those obtained using 500 images and a spring constant of 50 eV Å^{-2}. The initial and final states were found via energy minimization using the LBGFS[33] algorithm.

2.3. Accelerated Molecular Dynamics. Molecular dynamics is often used to generate the configurations employed for the calculations of the conductance of the system. However, the rotational barriers found between the dithiol conformers, of the order of a few tenths of eV, would preclude a thorough sampling of the different configurations via this method. To avoid this problem and enhance the sampling of the molecular conformers, the hyperdynamics method, as developed by Voter[34] et al. is applied here. This method is aimed to accelerate the exploration of a system undergoing rare events, without loosing its natural dynamics. The key is to transform the potential energy surface (PES) of the system $V(r)$ with the addition of a bias function ΔV_b, as shown in eq 1.

$$V_b(\mathbf{r}) = V(\mathbf{r}) + \Delta V_b(\mathbf{r}) \tag{1}$$

This transformation reduces the energy barriers of the system, making the residence time in the trapping minima shorter and allowing an efficient sampling of the configuration space in a reasonable simulation time. However, to recover the average of any time-dependent property (say A), such as molecular conductance, the sampled configuration must be reweighted using a proper factor (say w) that depends on the extent of the applied bias. Thus, the average property in the unbiased sampling ($\langle A\rangle_V$) is calculated from

$$\langle A\rangle_V = \langle Aw(r)\rangle_{V_b} \text{ where } w(r) = \frac{e^{\beta\Delta V_b(r)}}{\langle e^{\beta\Delta V_b(r)}\rangle_{V_b}} \tag{2}$$

where $\langle\ \rangle_{V_b}$ denote the average taking along the biased sampling.

According to Voter,[34] real time can be recovered through this reweighting, but an extra restriction must be added: the bias must vanish at the transition states (TS). However, this restriction is not required for the calculation of thermodynamic properties, as is the case of the conductance. Therefore, for any

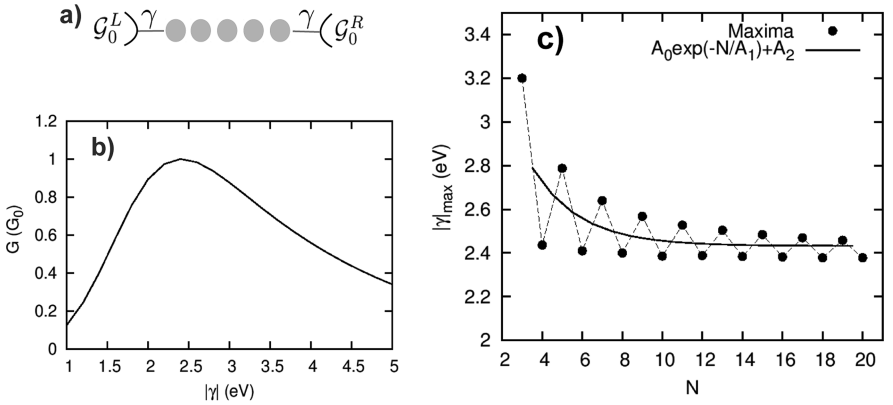

Figure 2. (a) Theoretical setup used to fit the γ parameter: five Au atoms wire coupled to two electron reservoirs using WBA. (b) Plot of conductance (in units of $2e^2/h$) as a function of parameter γ. (c) Plot γ_{max} as a function of the number of atoms in the chain (N). The fit of the average points with an exponential decay function is also shown. A_0 = 1.56, A_1 = 2.38, A_2 = 2.43.

bias function that allows a good sampling of the PES (i.e., maintaining the underlying shape) the reweighting equation is usable. For the present simulations, we employ the bias function proposed by Hamelberg et al.[35] given in eq 3.

$$\Delta V_b(\mathbf{r}) = \begin{cases} \dfrac{E - V(\mathbf{r})}{\alpha + E - V(\mathbf{r})} & V(\mathbf{r}) \le E \\ 0 & V(\mathbf{r}) \ge E \end{cases} \tag{3}$$

where E and α are tunable parameters. E is the threshold boost energy, since the boost is switched on when the system energy is below E. On the other hand, α regulates the deformation of the potential energy inside the basin.

To enhance the sampling of the different molecular conformers we applied the bias function to the torsional and 1−4 Lennard-Jones terms of the molecular potential as suggested by Hamelberg et al.[35] In this work we use a value of $E = 5.0 + \langle V[r(t_i)]\rangle$ eV (where $\langle V[r(t_i)]\rangle$ is the average energy) and α = 10.0 eV. These values were chosen after performing test simulations with different combinations of these parameters in the sets $E - \langle V[r(t_i)]\rangle = \{0.5,1.0,2.5,5\}$ eV and $\alpha = \{0.1,1,10\}$ eV. The selection was made for the set yielding the best linear correlation between the boosted time and the unboosted time (see refs 34 and 36), being the torsional barrier of the force field reduced to values that allow a proper sampling (of the order of 0.1 eV).

2.4. Conductance. The current flowing through the molecule coupled to two electron reservoirs (leads) is calculated by applying the Landauer−Büttiker formula,[37,38] which reads as given in eq 4.

$$I = \frac{2e}{h}\int_{\mu_L}^{\mu_R} T(\varepsilon)\, d\varepsilon \tag{4}$$

where the transmission function T is calculated using the Fisher−Lee formula,[39] eq 5.

$$T = Tr(\mathcal{G}^{+}_{dev}(\varepsilon)\Gamma_L(\varepsilon)\mathcal{G}^{-}_{dev}(\varepsilon)\Gamma_R(\varepsilon)) \tag{5}$$

In eq 5, $\mathcal{G}$ stands for the nonequilibrium Green function (NEGF) operator[40] of the device. This operator can be written as shown in eq 6.

$$\mathcal{G}_{dev}(z) = (zS - H_{dev} - \Sigma_L(z) - \Sigma_R(z))^{-1} \tag{6}$$

where S and H_{dev} are the overlap and Hamiltonian matrix of the device and z is referred to a complex energy. $\Sigma_L/R(z)$ are the self-energies for the left and right lead, respectively. The electronic structure of the device is determined using a semiempirical extended-Hückel (EH) Hamiltonian (H_{dev}). EH combined with NEGF has proven to be a useful tool for studying the complex relation between molecular structure and transport properties.[41,42] The simplicity of this Hamiltonian allows the calculations to become computationally affordable when dealing with large systems and when statistically significant number of G values needs to be probed all along the MD trajectories, as it is the case in the present work. In the Fisher-Lee formula for transmission, $\mathcal{G}^{+}_{dev}(z)$ is the advanced Green function operator for the system that consists of the device attached to one-dimensional leads (see Figure 2). μ_L and μ_R are the Fermi levels for the left and right electrodes, respectively, and $\Gamma_{L/R} = (\sum^{+}_{L/R}(z) - \Gamma^{-}_{L/R}(z))$. When expanded in a localized atomic orbital basis set, the matrix representation of $\Sigma_{L/R}$ that have nonzero elements are $(\Sigma_L)_{11} = \gamma^2\mathcal{G}_0^{+L}(z)$ and $(\Sigma_R)_{NN} = \gamma^2\mathcal{G}_0^{+R}(z)$ where block indexes 11 and NN stands for all the Au orbitals that are attached to the left and right leads respectively. In the present work all "s", "p" and "d" Au Hückel orbitals are considered to be equally coupled to the leads through the parameter γ. $\mathcal{G}_0^{+L/R}$ stands for the Green function operator for the left and right contacts respectively.[43] This contacts are modeled by semiinfinite one-dimensional nanowires represented within a nearest neighbor single hopping TB model (one orbital per site) with a coupling constant β. In the present work, a total of 274 leads were used to contact the Au atoms laying in the outermost planes of the surface slab and the tip. After applying the wide band approximation (WBA), $\mathcal{G}_0^{+L/R} = -\frac{i}{|\beta|}$. For all the calculations described below an arbitrary value of β = −3.88 eV was used. All the conductance calculations were performed at 0 V, hence, $G = (2e^2/h)T(\varepsilon_F)$, where the transmission function is evaluated at the device Fermi level ε_F.

To get conductance values that can be directly compared with experimental results, we have applied a fitting procedure to determine the optimal value of the molecule-contact coupling (parameter γ). This parameter was fitted to get $G = G_0 = 2e^2/h$ for several benchmark selected single atom metallic wires and was further used to represent the contact-device of the present work. This is, as far as we know, the first time that such a procedure is applied. A full investigation of this methodology will be the subject of an upcoming work.

dx.doi.org/10.1021/ct3007327 | J. Chem. Theory Comput. 2012, 8, 4539−4545

Figure 2a shows the present model setup built when a five Au atom chain is coupled with two electron reservoirs, as explained before. Figure 2b shows the plot of G vs γ that exhibits a maximum at $\gamma = -2.41$ eV. As this maximum slightly varies with the length of the chain and with the parity of the number of atoms,[44] calculations for various lengths were performed (Figure 2c). The average γ_{max} that results from the extrapolation to an infinite chain length is $\gamma = -2.43$ eV.

3. RESULTS

3.1. Static Lifting of a Dithiol Molecule. According to the experimental result reported in ref 14, conductance jumps found in $I(t)$ experiments are due to the spontaneous jump of a molecule, bridging the gap between the surface of the substrate and the STM tip. Thus, before addressing the dynamic calculation of conductances, we present a set of static calculations that should give an idea of the energy barriers found for the molecular jump. Activation energies and minimum energy paths were obtained from nudged elastic band (NEB) calculations.[32] The initial state of the system was the molecule adsorbed on the surface, and the final state was the molecule bridging the tip−surface gap. These results are presented in Figure 3.

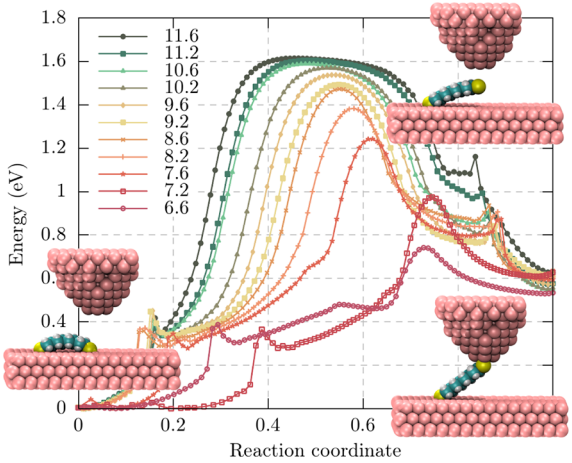

Figure 3. Potential energy vs reaction coordinate for the event of a molecular jump from the surface to the tip as obtained from NEB calculations at different tip−surface distances, given in Å in the figure. The insets correspond to the initial (bottom left), transition (top right), and final (bottom right) states of the curve for 11.6 Å.

While the energy-distance curves are smooth for large jump distances, those for short distances present some sharp features close to the position of the initial and final states. A close inspection of the NEB images corresponding to these features provides an explanation for their occurrence. As the dithiol molecule is dragged, its tail, in permanent contact with the surface, jumps between different hollow sites on the surface. Thus, the sudden jump between two neighboring hollow sites yields the secondary maxima observed (a set of movies is provided as Supporting Information).

From the NEB calculations (see dashed line of Figure 4), it is found that, for surface−tip distances ranging between 6.5 Å and 12 Å, the activation energy changes from 0.7 eV to somewhat more than 1.6 eV. These values are in good agreement with calculations previously reported by some of us using a more simplistic model.[45] However, it must be pointed out that the

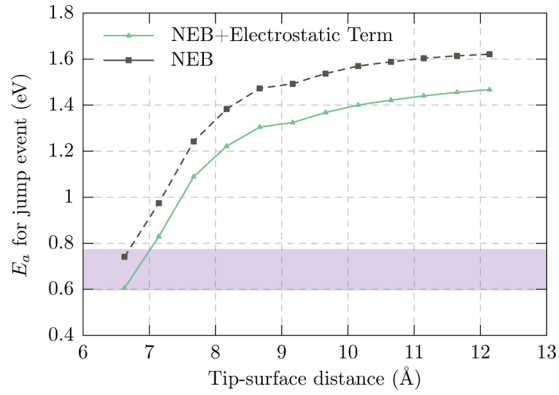

Figure 4. Activation energy for a molecular jump, as a function of the tip−surface distance with (solid line) and without (dashed line) consideration of an electrostatic field acting on the thiolate group. The charge assumed to be present on the thiolate group was $q_{thiolate} = -1\ e_0$ and the tip potential was $U_{tip} = +0.6$ V. The shadowed area denotes the activation energy range estimated for events occurring between 1 ms and 1s according to absolute-rate theory using a pre-exponential factor of 10^{13}. The temperature assumed was 300 K.

interatomic potential used here has an important number of improvements with respect to the one used in the aforementioned work. Furthermore, the minimum energy curves presented here were obtained using the NEB algorithm and not simply by lifting the molecule from the surface, as it was the case of the previous work.

We turn now to consider a factor that may decrease the energy barrier of the molecular jump. In ref 14, it was found that a 5-fold increase in the tip potential led to a larger rate of jump events. This was attributed to the increased electric field present in the tunnelling gap at higher tip potentials. To check this hypothesis, we calculated an upper bound of the electrostatic work due to the presence of the tip−surface field in a simple way. Denoting with Δz the distance between the closest Au atoms belonging to the tip and the surface respectively, and assuming that a charge $q_{thiolate}$ is present at the free thiolate unit, the work performed on the molecule by the field $(U_{tip}/\Delta z)$ at the gap may be approximated as

$$w(z) = \frac{U_{tip}}{\Delta z} z_{ss} q_{thiolate} \tag{7}$$

where z_{ss} is the z projection of the distance of the jumping sulfur atom measured with respect to its initial position. Assuming a large value of $q_{thiolate} = -1\ e_0$ and a typical $U_{tip} = +0.6$ V, we can add $w(z)$ to reaction coordinate. The potential energy barriers for the jumps under these conditions are shown in Figure 4. It is found that the electric field in the junction may cause some decrease in the jump barrier. However, the decrease obtained is still too small to provide an explanation for the occurrence of the molecular jumps observed experimentally. Furthermore, recent experiments show that the jump events still occur with a negative tip bias.[23]

3.2. Conformational Arrangement of a Dithiol Molecule. Accelerated dynamics (AD) simulations were performed at different tip−surface distances (Δz) in order to obtain information on the configuration of the molecule for different substrate−tip distances. Δz was varied between 5.7 Å and 15.5 Å, and the S−S distance was computed and referred to the all-trans conformation. These results are shown in Figure 5. There, it can be observed that, although the system explores

dx.doi.org/10.1021/ct3007327 | J. Chem. Theory Comput. 2012, 8, 4539−4545

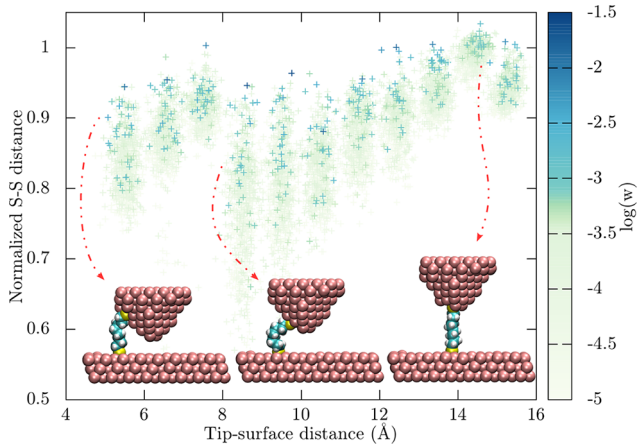

Figure 5. Normalized S−S distance vs the tip−surface distance. The former is referred to the all-trans conformation. The latter is calculated from the closest distance between Au atoms belonging to the tip and the surface, respectively. Point are colored according to their weight factor as obtained from the acelerated dynamics, the scale for which is located at the right of the plot.

some configurations where the molecule is compressed, these configurations seldom occur during the simulation. These results are different from those obtained from models that address conductance calculations by confining the molecule at distances considerably shorter than those corresponding to its complete elongation (as in ref 27), since this configuration implies that a very short S−S distance will be avoided by the effect shown in the previous figure. Whenever confined to a gap shorter than its length, the molecule will try to keep a more elongated form by sliding along the STM tip. This effect prevents strong changes in the conductance caused by extreme compression, as it is experimentally observed.

Although the average S−S distance experiments small changes for the elongated configurations occurring at large tip−surface distances, it is worth mentioning that under these conditions the scattering around the average S−S distance values becomes considerably smaller (see Figure S1 of the Supporting Information). This is due to the fact that larger surface−tip distances tend to generate stretched molecular configurations, where sulfur atoms are more restricted around an average position.

3.3. Conductance Calculations. Conductances were calculated for configurations sampled through the accelerated dynamics procedure discussed above for different tip−surface distances. Figure 6 shows two typical conductance histograms obtained from configurations sampled through the accelerated dynamics procedure discussed above for different tip−surface distances at different distances. For the case where Δz = 9.5 Å, a single conductance maximum is observed around 2.5 × 10^{-6} G/G_0. A similar qualitative behavior is observed for all histograms between Δz = 6.5 Å and Δz = 15.5 Å. For the case where Δz = 5.7 Å, two contributions clearly arise in the conductance. One of the order of 10^{-5} G/G_0 and another in the range between 10^{-3} and 1 G/G_0. This remarkable behavior led us to analyze the different simulations frames at this distance, with the finding that when the tip is close to the surface, a singular configurations appears (see the movies in the Supporting Information). It comes out that although the molecule drifts outside the junction most of the time to avoid highly twisted configurations (see Figure 5), in some of the

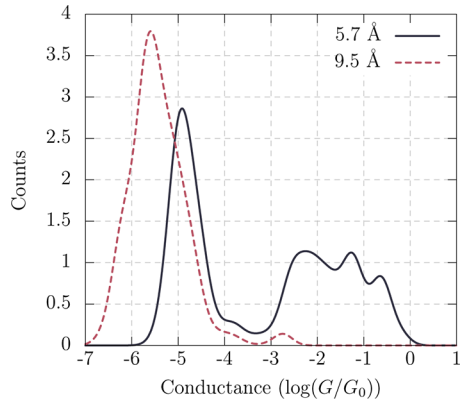

Figure 6. Typical histograms of logarithmic conductance at two tip−surface distances (5.7 and 9.5 Å).

sampled structures one of the molecular ends becomes interposed in the gap. This configuration, which is shown in Figure 7 and exhibits conductivities that are typically 3 to 4 orders of magnitude larger than the previous ones, appears (and disappears) spontaneously during the simulations.

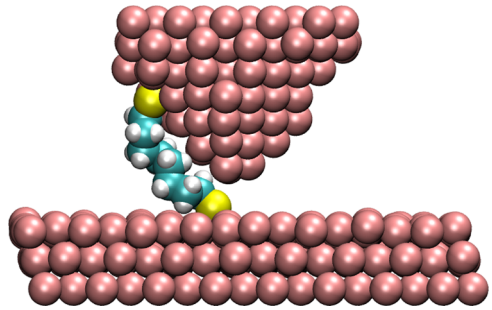

Figure 7. Snapshot of a simulation where the bottom end of the dithiol molecule becomes interposed in the tip−metal junction, generating a configuration with a high conductance value.

Besides the S−S distance, we found it useful to characterize the structure of the thiol by what we will call the dihedral signature Θ_S, defined as

$$\Theta_S = \frac{1}{\pi}\sum_{i=1}^{n} |\theta_i| \tag{8}$$

where θ_i is the ith dihedral angle of the molecule. In the case of the octanedithiol molecule, the sum is taken over the seven main dihedral angles (five of these angles are calculated considering four consecutive C atoms groups, and two of them are built taking groups of three C and the S consecutive atom). Each dihedral angle has a value of $\pm\pi$ in the trans configuration and 0 in the cis configuration (see Scheme 1). Thus, Θ_S may take values between 0 and 7 for octanedithiol, corresponding to

Scheme 1. Convention Used in This Work for Dihedral Angle Values

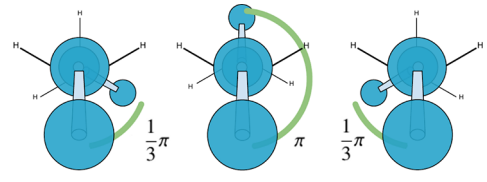

dx.doi.org/10.1021/ct3007327 | J. Chem. Theory Comput. 2012, 8, 4539−4545

the all cis (hypothetical) and all trans configurations, respectively. This parameter reflects in some way, as the S−S distance does, the twisting state of the molecule (the correlation found between these parameters is shown in the Supporting Information).

To analyze the correlation between molecule conformation and the conductance of the system, Figure 8 shows an scatter

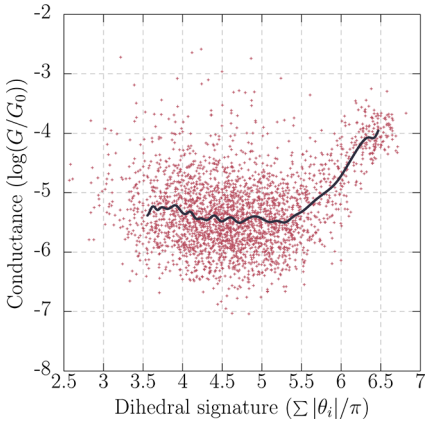

Figure 8. Scatter plot of conductance as a function of dihedral signature containing data collected for all tip−surface distances. The solid line is only a guide to the eye, obtained from a Bezier smoothing of the data points.

plot of conductance vs dihedral signature that contains the data collected for all tip−surface distances. It is found that G increases from 10^{-6} to 10^{-4} when the molecular twist (Θ_S) changes from 4 to 7. These results show that the elongated molecule presents a larger conductance than a twisted one under the present simulation conditions. This appears to be in contradiction with the results of Jones et al.,[27] where it was found that conductance seems to decrease with the progressive elongation of the molecule. However, in that work, sampled configurations were obtained by confining the molecule in the gap between two metal surfaces, and the mentioned conductance drop was found for relative S−S distances between 0.3 and 0.8. However, in the present simulations, conditions the molecule cannot be forced to low S−S distances, and only a conductance increase is found, as was also shown by Jones et al., for relative S−S distances larger than 0.9.

Average conductances were calculated for different tip−surface distances. These results are presented in Figure 9. This figure shows that the conductance increases at relatively short and long distances, with a minimum at intermediate Δz values. This behavior of the conductance can be understood in terms of the discussion given above. When the tip is drawn close to the surface, the configurations in which the sulfur atom bridges the substrate−tip gap for electron transport start to deliver an increasing contribution to the conductance. This is the reason for the increase in the conductance values in our model. On the other end of the plot, when the tip becomes more distant from the surface, the increase in the conductance is due to the improved electronic transport through the molecule due to its prominently all-trans conformation (see Figure 6). While the first effect has been observed (see the Supporting Information of ref 23), the latter has so far not been reported. This is probably due to the spontaneous detachment of the molecule when it becomes subject to the relatively large forces required to obtained more stretched configurations. However, in some

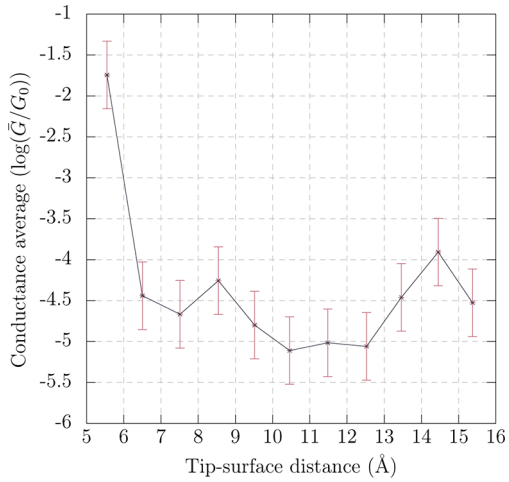

Figure 9. Average of conductance calculation for different tip−surface distances Δz. Each point was obtained from a set of 200 NEGF calculations with configuration taken from accelerated dynamics simulations.

experiments, such as those shown in Figure 4 of ref 14, some nonmonotonic I vs stretching-distance curves are found. This may be an indication for the increase of conductivity of the molecular junction upon stretching. The reason for this is that the extended configuration has an easier path for electron transmission where both highest occupied (HOMO) and lowest unoccupied (LUMO) molecular orbitals, the main responsible for electronic transmission, have an uninterrupted electron density projection connecting both sulfur atoms (see the Supporting Information).

A comment must be added when comparison of the present results is attempted with experiment, such as those presented in ref 23. The present theoretical results should, in principle, be valid for experiments performed in vacuum, while experiments are usually performed in air or in the liquid phase. These different conditions represent strongly different situations for electron tunnelling. For example, in ref 23, the reported value of the slope $d\ \ln(I)/ds$ (I tunnelling current, s absolute tip sample separation) is $10 \pm 1.5\ \text{nm}^{-1}$, resulting an effective barrier of the order of 1 eV. On the other hand, experiments in UHV for a Au(111) surface yield barriers of the order of 3.6 eV.[46] Whatever the reason for the relatively low values obtained for the measurements in air, this will result in an increased penetration of the electrons in the gap. This would bear consequences in the effect predicted here at short tunnelling distances. Thus, the effect of increased conductance due to the sulfur intercalation in the gap will be probably observed in experiment at larger distances than those predicted from the present calculations.

3.4. Conclusions. The present work tackles by means of computer simulations the study of the behavior of a dithiol molecule confined at the gap between a metal tip and a perfect metal surface. For the first time, conductance calculations for this system are made using configurations sampled from an accelerated molecular dynamics procedure. Furthermore, the sulfur−metal interaction is modeled using a semiepirical potential fitted from first-principles calculations. It is found that although the present one is one of the most simple systems conceivable (the surface is completely absent from defects), singular molecular configurations may lead to increased conductances at short tip−surface distances. Application of

dx.doi.org/10.1021/ct3007327 | J. Chem. Theory Comput. 2012, 8, 4539−4545

similar simulation schemes may be useful to understand the multiplicity of conductance components found for more complex systems, involving surfaces with different types of defects. An interesting question arising from the present work is also the fact that the barrier estimated for the molecular jump between the surface and the tip would set times for the jumps far beyond those observed experimentally. This fact also provides an interesting motivation for future theoretical studies.

■ ASSOCIATED CONTENT

Supporting Information

Correlation between dihedral signature and S−S distance (Figure S1); HOMO and LUMO orbital screenshots for twisted and elongated molecular configuration (Figure S2); three movies that show the minimum reaction path for molecular jump events at different tip−surfaces distances; one movie in which MD and AD simulations are compared by means of the dihedral signature and S−S distance parameters; and one movie that shows how one end of the molecule is interposed between the tip and the supeficie. This material is available free of charge via the Internet at http://pubs.acs.org/.

■ AUTHOR INFORMATION

Corresponding Author

*E-mail: eleiva@fcq.unc.edu.ar.

Notes

The authors declare no competing financial interest.

■ ACKNOWLEDGMENTS

We acknowledge financial support from CONICET PIP 112-200801-000983, Secyt Universidad Nacional de Córdoba, Program BID (PICT-BICENTENARIO-2010-123), and PME 2006-01581.

■ REFERENCES

(1) Aviram, A.; Ratner, M. *Chem. Phys. Lett.* **1974**, *29*, 277−283.
(2) Wang, K.; Rangel, N. L.; Kundu, S.; Sotelo, J. C.; Tovar, R. M.; Seminario, J. M.; Liang, H. *J. Am. Chem. Soc.* **2009**, *131*, 10447−51.
(3) Negre, C. F. A.; Sánchez, C. G. *J. Chem. Phys.* **2008**, *129*, 034710.
(4) Haiss, W.; van Zalinge, H.; Higgins, S. J.; Bethell, D.; Höbenreich, H.; Schiffrin, D. J.; Nichols, R. *J. Am. Chem. Soc.* **2003**, *125*, 15294−15295.
(5) Olmos, J.; Mariscal, M.; Leiva, E. *Electrochim. Acta* **2009**, *54*, 2977−2982.
(6) Quek, S. Y.; Kamenetska, M.; Steigerwald, M.; Choi, H. J.; Louie, S. G.; Hybertsen, M. S.; Neaton, J. B.; Venkataraman, L. *Nat. Nanotechnol.* **2009**, *4*, 230−234.
(7) Chen, F.; Hihath, J.; Huang, Z.; Li, X.; Tao, N. J. *Annu. Rev. Phys. Chem.* **2007**, *58*, 535−564.
(8) Tao, N. J. *Nat. Nanotechnol.* **2006**, *1*, 173−181.
(9) Guo, S.; Hihath, J.; Dez-Pérez, I.; Tao, N. *J. Am. Chem. Soc.* **2011**, *133*, 19189−97.
(10) Makk, P.; Tomaszewski, D.; Martinek, J.; Balogh, Z.; Csonka, S.; Wawrzyniak, M.; Frei, M.; Venkataraman, L.; Halbritter, A. *ACS Nano* **2012**, *6*, 3411−23.
(11) Nichols, R. J.; Haiss, W.; Higgins, S. J.; Leary, E.; Martin, S.; Bethell, D. *Phys. Chem. Chem. Phys.* **2010**, 2801−2815.
(12) Li, C.; Pobelov, I.; Wandlowski, T.; Bagrets, A.; Arnold, A.; Evers, F. *J. Am. Chem. Soc.* **2008**, *130*, 318−26.
(13) Xu, B.; Tao, N. J. *Science* **2003**, *301*, 1221−1223.
(14) Haiss, W.; Nichols, R. J.; van Zalinge, H.; Higgins, S. J.; Bethell, D.; Schiffrin, D. J. *Phys. Chem. Chem. Phys.* **2004**, *6*, 4330−4337.
(15) Li, X.; He, J.; Hihath, J.; Xu, B.; Lindsay, S. M.; Tao, n. *J. Am. Chem. Soc.* **2006**, *128*, 2135−2141.
(16) Dadosh, T.; Gordin, Y.; Krahne, R.; Khivrich, I.; Mahalu, D.; Frydman, V.; Sperling, J.; Yacoby, A.; Joseph, I. B. *Nature* **2005**, *436*, 677.
(17) Kergueris, C.; Bourgoin, J.; Palacin, S.; Esteve, D.; Urbina, C.; Magoga, M.; Joachim, C. *Phys. Rev. B* **1999**, *59*, 505−513.
(18) Vélez, P.; Dassie, S.; Leiva, E. P. M. *Phys. Rev. Lett.* **2005**, *95*, 045503.
(19) Vélez, P.; Dassie, S.; Leiva, E. P. M. *Chem. Phys. Lett.* **2008**, *460*, 261−265.
(20) Vélez, P.; Dassie, S.; Leiva, E. P. M. *Phys. Rev. B* **2010**, *81*, 235435.
(21) Michoff, M. E. Z.; Velez, P.; Leiva, E. P. *J. Phys. Chem. C* **2009**, *113*, 3850−3854.
(22) *Recent Advances in Nanoscience*; Mariscal, M., Dassie, S. A., Eds.; Research Signpost: Scarborough, Ontario, 2007.
(23) Haiss, W.; Martin, S.; Leary, E.; van Zalinge, H.; Higgins, S. J.; Bouffier, L.; Nichols, R. *J. Phys. Chem. C* **2009**, *113*, 5823−5833.
(24) Kornyshev, A. A.; Kuznetsov, A. M. *Chem. Phys.* **2006**, *324*, 276−279.
(25) Kornyshev, A. A.; Kuznetsov, A. M.; Ulstrup, J. *Proc. Natl. Acad. Sci. U.S.A.* **2006**, *103*, 6799−804.
(26) Paulson, M.; Krag, C.; Frederiksen, T.; Brandbyge, M. *Nano Lett.* **2009**, *9*, 117−121.
(27) Jones, D.; Troisi, A. *J. Phys. Chem. C* **2007**, *111*, 14567−14573.
(28) Andrews, D. Q.; Van Duyne, R. P.; Ratner, M. A. *Nano Lett.* **2008**, *8*, 1120−6.
(29) Olmos-Asar, J.; Rapallo, A.; Mariscal, M. *Phys. Chem. Chem. Phys.* **2011**, *13*, 6500−6506.
(30) Siu, S. W. I.; Pluhackova, K.; Böckmann, R. A. *J. Chem. Theory Comput.* **2012**, *8*, 1459−1470.
(31) Bulou, H.; Massobrio, C. *Phys. Rev. B* **2005**, *72*, 205427.
(32) Henkelman, G.; Jonsson, H. *J. Chem. Phys.* **2000**, *113*, 9978.
(33) Zhu, C.; Byrd, R.; Lu, P.; Nocedal, J. *ACM Trans. Math. Software* **1997**, *23*, 550−560.
(34) Voter, A. F. *J. Chem. Phys.* **1997**, *106*, 11.
(35) Hamelberg, D.; Mongan, J.; McCammon, J. A. *J. Chem. Phys.* **2004**, *120*, 11919−29.
(36) Pal, S.; Fichthorn, K. A. *Chem. Eng. J.* **1999**, *74*, 77−83.
(37) Landauer, R. *Philos. Mag.* **1970**, *21*, 873.
(38) Büttiker, M. *Phys. Rev. Lett.* **1986**, *57*, 1761.
(39) Fisher, D. S.; Lee, P. A. *Phys. Rev. B* **1981**, *23*, 6851−6854.
(40) Xue, Y.; Datta, S.; Ratner, M. A. *Chem. Phys.* **2002**, *281*, 151−170.
(41) Andrews, D. Q.; Cohen, R.; Van Duyne, R. P.; Ratner, M. A. *J. Chem. Phys.* **2006**, *125*, 174718.
(42) Negre, C. F. A.; Jara, G. E.; Vera, D. M. A.; Pierini, A. B.; Sánchez, C. G. *J. Phys.: Cond. Matt.* **2011**, *23*, 245305.
(43) Todorov, T. N.; Briggs, G. A. D.; Sutton, A. P. *J. Phys.: Condens. Matter* **1993**, *5*, 2389−2406.
(44) Major, P.; García-Suárez, V. M.; Sirichantaropass, S.; Cserti, J.; Lambert, C. J.; Ferrer, J. *Phys. Rev. B* **2006**, *73*, 45421.
(45) Olmos, J.; Leiva, E.; Mariscal, M. *Electrochem. Commun.* **2009**, *11*, 987−989.
(46) Yamada, Y.; Sinsarp, A.; Sasaki, M.; Yamamoto, S. *Jpn. J. Appl. Phys.* **2003**, *42*, 4898−4900.